ChemComm

Accepted Manuscript

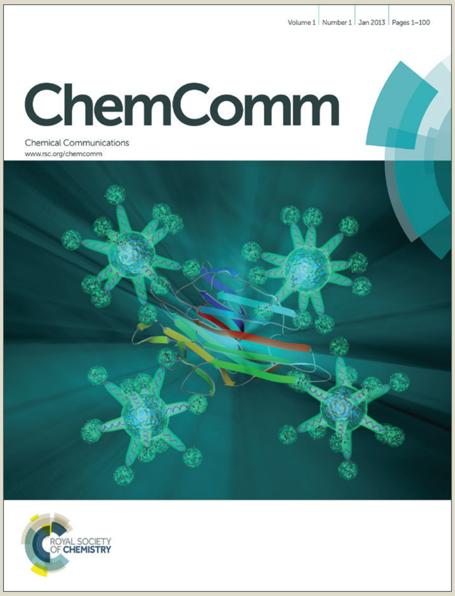

ROYAL SOCIETY OF CHEMISTRY

www.rsc.org/chemcomm

ChemComm

Dynamic Article Links ►

Cite this: DOI: 10.1039/c0xx00000x

www.rsc.org/xxxxxx

COMMUNICATION

Significant promotion effect of carbon nanotubes on the electrocatalytic activity of supported Pd NPs for ethanol oxidation reaction of fuel cells: The role of inner tubes†

Jin Zhang[a], Yi Cheng[a], Shanfu Lu[b], Lichao Jia[a], Pei Kang Shen[c] and San Ping Jiang*[a]

Received (in XXX, XXX) Xth XXXXXXXXX 20XX, Accepted Xth XXXXXXXXX 20XX
DOI: 10.1039/b000000x

The inner tubes of carbon nanotubes (CNTs) have significant promotion effect on the electrocatalytic activity of Pd nanoparticles (NPs) on the ethanol oxidation of direct alcohol fuel cells (DAFCs) and Pd NPs supported on CNTs with 3-7 walls show a much higher activity as compared to that supported on typical single-walled and multi-walled CNTs.

Carbon nanotubes (CNTs) are the most common and superior supports for precious metal-based electrocatalysts such as Pt, Pd, PtRu mainly because of their excellent conductivity, ultrahigh surface area and good chemical, thermal and structural stability.[1, 2] Moreover, graphitized CNTs are intrinsically resistance to corrosion in favour of supporting metal catalysts in acid as well as alkaline environment.[3] CNTs also provide high catalyst dispersion and promote electron transfer in the catalyst layer, enhancing the electrocatalytic activity of metal catalyst.[4] However, although it has been well established that doping of CNTs with nitrogen substantially enhances the electrocatalytic activity of CNTs for fuel cell reactions such as oxygen reduction reactions,[5, 6] it is generally believed that pristine CNTs without nitrogen-doping have little electrocatalytic activity since the active sites of edge plane exposure alone are far too low for the electrochemical reactions of fuel cells.[6-8]

Most recently, we showed that pristine CNTs composed of between 2-7 concentric tubes or walls have an outstanding activity for the O_2 evolution reaction (OER) in alkaline solutions as compared with typical single-walled and multi-walled CNTs (SWNTs & MWNTs).[9] The results indicate that the outstanding activity of pristine CNTs for OER is most likely originated from the effective electron transfer between the outer wall and inner tubes of CNTs. For the OER on CNTs with specific number of walls, efficient electron transfer could occur on the inner tubes of the CNTs most likely through electron tunnelling between outer wall and inner tubes under the electrochemical polarization driving force, significantly promoting the charge transfer reaction of OER at the surface of outer wall of the CNTs. Such promotion effect of inner tubes of CNTs for the charge transfer process implies the possible activation effect on the electrocatalytic activity of supported precious metal catalysts for alcohol oxidation of fuel cells. To verify this hypothesis, we selected Pd nanoparticles (NPs) as model catalysts for the ethanol oxidation reactions (EOR) of direct alcohol fuel cells (DAFCs).

Pd is the promising potential substitute for Pt-based catalysts in the DAFCs because of the low cost and relatively high abundant resources on earth in comparison with Pt.[10, 11] Moreover, Pd shows higher alcohol oxidation activity and higher CO poisoning resistance than Pt in alkaline solutions due to the low desorption energy of CO on the surface of Pd.[12-14] Herein, Pd NPs with similar particle size were uniformly assembled on the outer wall surface of selected CNTs with average number of walls of 1, 3, 7 and 12 and the electrocatalytic activity of Pd NPs supported on CNTs was investigated for EOR in alkaline solutions. The electrocatalytic activity of Pd NPs supported on CNTs showed a distinctive volcano-type dependence on the number of walls of CNT supports and the highest electrocatlaytic activity was obtained on Pd NPs supported on CNTs with average 3-7 walls.

Figure 1 is the TEM micrographs of the CNT supports used in this study. CNTs were purified by ultrasonic treatment in concentrated HCl solution before use. After purification, the amount of Fe, Co, Mo and Ni elements are substantially reduced to less than 100 ppm as confirmed by the ICP-OES analysis (Table S1, ESI†). CNTs-1 mainly consists of SWNTs (79%) with outer diameter of 1.97 nm. CNTs-2 is dominated by triple-walled CNTs (TWNTs, 52%) with outer diameter of 3.80 nm. The average number of walls of CNTs-3 is 7 with outer diameter of 7.45 nm, while CNTs-4 is a typical MWNT with average 12 walls and outer diameter of 13.9 nm. CNTs with small outer diameter prefers to form bundles (marked by the circles in Fig.1A and B) because of the van der Waals interactions;[15] however, CNTs with large outer diameters, CNTs-3 and CNTs-4, are dispersed well without bundles. Raman spectroscopy analysis shows that the intensity ratio of defect-derived D band (I_D) to graphite-derived G band (I_G), I_D/I_G, is 0.16 for CNTs-1 (Fig.S1,

---

[a] *Fuels and Energy Technology Institute & Department of Chemical Engineering, Curtin University, Perth, WA 6102, Australia. E-mail: s.jiang@curtin.edu.au (SP Jiang).*
[b] *School of Chemistry and Environment, Beihang University, Beijing 100191, China*
[c] *Advanced Energy Materials Research Laboratory, School of Physics and Engineering, Sun Yat-sen University, Guangzhou 510275, China.*

† Electronic Supplementary Information (ESI) available: [The experimental section, ICP, Raman, BET, XPS, and supplementary results and discussion]. See DOI: 10.1039/b000000x/

ESI†), consistent that reported for SWNTs,[16] while the high I_D/I_G ratio of 2.5 for CNTs-4 shows that CNTs-4 is typical MWNTs with the high structural defects due to its multiple graphite layers.[17, 18]

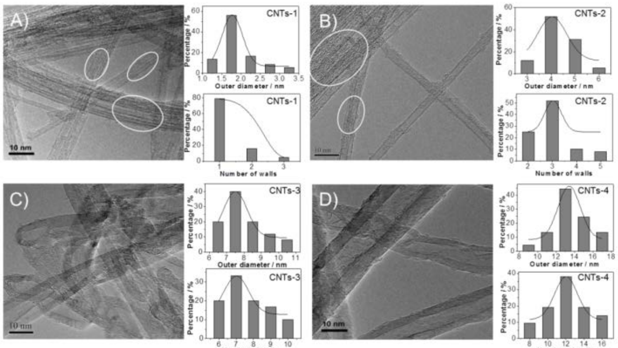

Fig.1 TEM images and related size and number of walls distribution of (A) CNTs-1, (B) CNTs-2, (C) CNTs-3 and (D) CNTs-4.

Pd NPs were dispersed uniformly on tetrahydrofuran (THF)-functionalized CNTs via self-assembly route.[19] Figure 2 is the TEM micrograph and XRD curves of Pd-CNTs. Pd NPs with diameter of 2.1 to 2.8 nm were homogeneously deposited on the surface of CNTs with no agglomeration, and the size is much smaller than 4.3 - 8.4 nm of Pd particles deposited on CNTs reported in the literature.[2, 20] This indicates that THF is an effective functionalization agent for CNT support. The distance between two lattice fringes of Pd NPs is 0.23 nm (Fig.2E), consistent with the *d*-spacing value of Pd (111) plane at 40.0 ° (Fig.2F). The peak at 25.9 ° is attributed to the hexagonal carbon structure of CNTs in (002) plane.[21] The peaks at 46.3 °, 67.8 ° and 80.6° correspond to Pd (200), Pd (220), and Pd (311), respectively. The XRD result confirms the face centred cubic (*fcc*) crystal structure of Pd NPs.[22] According to the Rietveld analysis in the XRD pattern, there is no preferred orientation effect on Pd NPs.

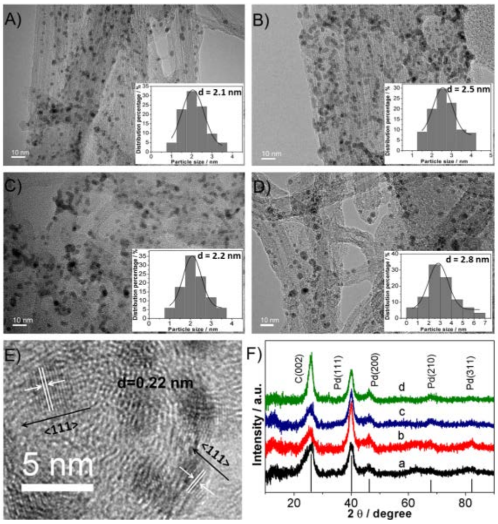

Fig.2 TEM micrographs and histograms of (A) Pd-CNTs-1; (B) Pd-CNTs-2; (C) Pd-CNTs-3; (D) Pd-CNTs-4.(E) HR-TEM image of Pd NPs and (F) XRD curves of (a) Pd-CNTs -1, (b) Pd-CNTs-2, (c) Pd-CNTs-3 and (d) Pd-CNTs-4.

The electrocatalytic activity of Pd-CNTs was evaluated for the EOR and the results are shown in Fig.3. Ethanol oxidation is characterized by well-separated anodic peaks in forward and reversed scans and the magnitude of the anodic current density in the forward scan is directly related to the amount of ethanol oxidized at Pd electrodes (Fig.3A). The electrocatalytic activity of Pd-CNTs strongly depends on the characteristics of CNTs supports and the best results were observed on Pd supported on CNTs-2, Pd-CNTs-2, achieving a peak current density of 2858 mA mg^{-1}. This is significantly higher than 1484 and 1574 mA mg^{-1} for Pd-CNTs-1 and Pd-CNTs-4, respectively. The onset potential for Pd-CNTs-2 is 0.353 V, which is also more negative than 0.400 and 0.394 V observed on Pd-CNTs-1 and Pd-CNTs-4, respectively. The electrocatalytic activity of Pd-CNTs-3 is slightly lower than that of Pd-CNTs-2, but significantly higher as compared to Pd-CNTs-1 and Pd-CNTs-4. Pd-CNT catalysts show a distinctive volcano-type dependence of the electrocatalytic activity as a function of number of walls of CNT supports (Fig.3B).

The electrochemical stability of Pd-CNTs for EOR was also investigated. The initial rapid decay in the current density for the ethanol oxidation on Pd catalysts indicates the poisoning of intermediates (Fig.3C), similar to the reaction on Pt electrodes in acid solution.[23] However, the current decay for the reaction on Pd-CNTs-2 and Pd-CNTs-3 is significantly slower than that on Pd-CNTs-1 and Pd-CNTs-4. The current density of Pd-CNTs at t=1000 s against the wall numbers of CNTs also shows a distinct volcano curves (Fig.3D). The results indicate that CNTs-2 and CNTs-3 support significantly promotes the tolerance and resistance of Pd NPs toward the poisoning effect of intermediate species of the EOR.

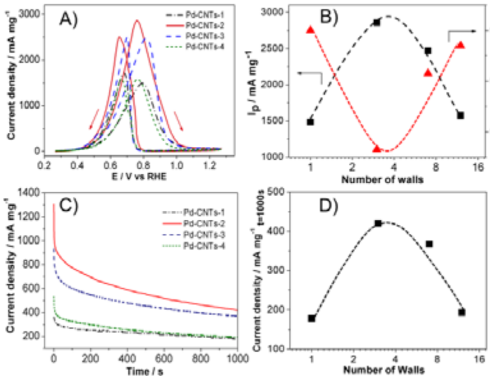

Fig.3 (A) Cyclic voltammetry curves of Pd-CNTs catalysts for EOR measured in a 1.0 M ethanol + 1.0 M KOH solution at scan rate 50 mV s^{-1}, (B) plots of peak current density and on set potential of EOR against wall numbers of CNTs, (C) chronoamperometry curves of Pd-CNTs catalysts for EOR, measured at 0.67 V in a 1.0 M ethanol + 1.0 M KOH solution, (D) plots of current density measured at t=1000 s for EOR. Pd loading was 0.05 mg cm^{-2}.

The high electrocatalytic activity of Pd NPs supported on CNTs with average 3-7 walls, Pd-CNTs-2 and Pd-CNTs-3, is not related to the particle size of Pd NPs or the surface area of CNTs. As shown in Fig.2, the average size of Pd NPs of Pd-CNTs-2 is 2.5 nm, higher than 2.1 nm for Pd-CNTs-1. Based on the N_2 adsorption isotherms the BET surface area of CNTs-1, CNTs-2, CNTs-3 and CNTs-4 is 576.7, 523.2, 538.8 and 270.6 m^2 g^{-1}, respectively. The surface area of CNTs-1 is much higher than

CNTs-4, but the electrocatalytic activity of Pd-CNTs-1 and Pd-CNTs-4 is very close. Also, the distinctive volcano-type relationship between the activity and number of walls of CNTs support cannot be attributed to the electronic interaction between the Pd NPs and CNTs nor the PdO content. XPS analysis indicates that the binding energy of $3d_{3/2}$ = 341.1 eV and $3d_{5/2}$ = 335.8 eV in Pd-CNTs is more or less the same, as compared with the standard spectra of metal Pd(0) (Fig.S2, ESI†). The content of PdO increases from 44.3 % to 67.3 % as the number of walls of CNTs increases from 1 to 12. PdO, like RuO_2, could donate oxygen to promote the oxidation of CO to CO_2, facilitating the EOR on Pd catalyst with high PdO content.[24] However, the activity of Pd-CNTs-4 is much lower than that of Pd-CNTs-2 despite its high PdO content of 67.3%. In addition, CNTs shows no activity for EOR (Fig.S3, ESI†), indicating that defects, surface functionalities or impurities of pristine CNTs used in the present studies have no electrocatalytic effect for the EOR.

The most significant finding of the present study is that the distinctive volcano-type curve observed for the electrocatalytic activity of Pd NPs (Fig.3) is exactly the same as that observed for the OER on pristine CNTs in alkaline solution (see Fig.4A).[9] Although the mechanism of the EOR in alkaline systems is still disputed, it is generally accepted that the EOR involves many intermediates (e.g., CH_3CO, CO),[25] similar to that reported in the acid solution.[26] As shown by Liang et al,[25] rate-determining step for EOR is the removal of the adsorbed ethoxi, CH_3CO_{ads}, by the adsorbed hydroxyl on the Pd electrode. The outstanding activity of CNTs with 2-7 concentric tubes or walls for OER indicates that the adsorption and migration or diffusion of oxygen-containing species, OH_{ads}, on the outer wall surface of CNTs is facile.[9] This would lead to the fast stripping of ethoxi and CO species via the interaction with OH_{ads}, releasing acetate as final product. Similar to OER on pristine CNTs, the intact inner-tube could serve as the effective electron conducting pathway for the EOR. The charge transfer could occur on the inner tubes through the electron tunnelling between the outer wall and inner tubes under the electrochemical polarization potential driving force. Such effective charge transfer process can effectively reduce the PdO/Pd-OH and release the active sites on Pd NPs for the reaction. Such charge transfer through electron tunnelling would not be possible with SWNTs and diminishes with the increase of the number of walls higher than 7 for typical MWNTs. Such promotion effect of inner tube on the EOR is schematically shown in Fig.4B.

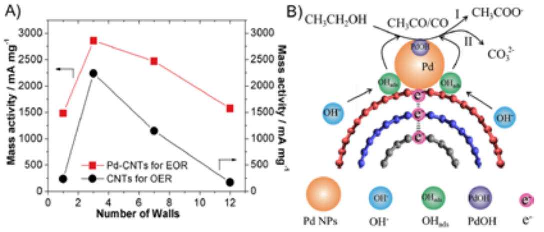

Fig.4 (A) Comparison of mass specific activity of Pd-CNTs catalysts for EOR and OER in alkaline solutions. The current density for OER was measured at 1.8 V vs RHE in 1 M KOH solution with scan rate of 1 mV s^{-1} and CNT loading of 0.025 mg cm^{-2}.[9] (B) Scheme of EOR on Pd-CNTs-2, facilitated by adsorption of oxygen containing species, OH_{ads} and charge transfer between outer wall and inner tubes via electron tunnelling under electrochemical polarization driving force.

In summary, we have demonstrated for the first time that electrocatalytic activity of Pd NPs depends critically on the number of inner tubes of CNT supports. The inner tubes of CNT support play an important role for EOR in the facilitation of adsorption and migration of oxygen-containing species and promotion of the charge transfer between outer wall and inner tube via electron tunnelling effect under electrochemical polarization potential.

This work is financially supported by the Australia Research Council (project number: DP120104932, DP120102325) and the Major International (Regional) Joint Research Project of NNSFC (5121002), China.

Notes and references

1 D. M. Guldi, G. M. A. Rahman, V. Sgobba, C. Ehli, *Chemical Society Reviews*, 2006, **35**, 471-487.
2 O. Winjobi, Z. Zhang, C. Liang, W. Li, *Electrochimica Acta*, 2010, **55**, 4217-4221.
3 C. C. Hung, P. Y. Lim, J. R. Chen, H. C. Shih, *Journal of Power Sources*, 2011, **196**, 140-146.
4 D. H. Nagaraju, G. S. Suresh, *ECS Electrochem. Lett.*, 2012, **1**, F21-F23.
5 K. P. Gong, F. Du, Z. H. Xia, M. Durstock, L. M. Dai, *Science*, 2009, **323**, 760-764.
6 S. Kundu, T. C. Nagaiah, W. Xia, Y. M. Wang, S. Van Dommele, J. H. Bitter, M. Santa, G. Grundmeier, M. Bron, W. Schuhmann, M. Muhler, *J. Phy. Chem. C*, 2009, **113**, 14302-14310.
7 I. Kruusenberg, N. Alexeyeva, K. Tammeveski, J. Kozlova, L. Matisen, V. Sammelselg, J. Solla-Gullon, J. M. Feliu, *Carbon*, 2011, **49**, 4031-4039.
8 R. Kannan, U. Bipinlal, S. Kurungot, V. K. Pillai, *Physical Chemistry Chemical Physics*, 2011, **13**, 10312-10317.
9 Y. Cheng, C. W. Xu, L. C. Jia, J. D. Gale, L. L. Zhang, C. Liu, P. K. Shen, S. P. Jiang, *Applied Catalysis B-Environmental*, 2015, **163**, 96-104.
10 J. Seweryn, A. Lewera, *J. Power Sources*, 2012, **205**, 264-271.
11 F. Kadirgan, S. Beyhan, T. Atilan, *Int. J. Hydrogen Energy*, 2009, **34**, 4312-4320.
12 C. W. Xu, H. Wang, P. K. Shen, S. P. Jiang, *Advanced Materials*, 2007, **19**, 4256-4259.
13 F. P. Hu, Z. Wang, Y. Li, C. Li, X. Zhang, P. K. Shen, *J. Power Sources*, 2008, **177**, 61-66.
14 G. Hu, F. Nitze, H. R. Barzegar, T. Sharifi, A. Mikolajczuk, C.-W. Tai, A. Borodzinski, T. Wagberg, *J. Power Sources*, 2012, **209**, 236-242.
15 T. Kim, G. Kim, W. I. Choi, Y.-K. Kwon, J.-M. Zuo, *Applied Physics Letters*, 2010, **96**.
16 V. M. Irurzun, M. P. Ruiz, D. E. Resasco, *Carbon*, 2010, **48**, 2873-2881.
17 A. M. Rao, S. Bandow, E. Richter, P. C. Eklund, *Thin Solid Films*, 1998, **331**, 141-147.
18 S. Costa, E. Borowiak-Palen, M. Kruszynska, A. Bachmatiuk, R. J. Kalenczuk, *Materials Science-Poland*, 2008, **26**, 433-441.
19 D. L. Wang, S. F. Lu, S. P. Jiang, *Electrochim. Acta*, 2010, **55**, 2964-2971.
20 V. Bambagioni, C. Bianchini, A. Marchionni, J. Filippi, F. Vizza, J. Teddy, P. Serp, M. Zhiani, *J. Power Sources*, 2009, **190**, 241-251.
21 W. Li, C. Liang, W. Zhou, J. Qiu, Zhou, G. Sun, Q. Xin, *The Journal of Physical Chemistry B*, 2003, **107**, 6292-6299.
22 R. D. Morgan, A. Salehi-khojin, R. I. Masel, *J. Phy. Chem. C*, 2011, **115**, 19413-19418.
23 E. Antolini, *J. Power Sources*, 2007, **170**, 1-12.
24 K. Ding, Y. Wang, H. Yang, C. Zheng, YanliCao, H. Wei, Y. Wang, Z. Guo, *Electrochim. Acta*, 2013, **100**, 147-156.
25 Z. X. Liang, T. S. Zhao, J. B. Xu, L. D. Zhu, *Electrochim. Acta*, 2009, **54**, 2203-2208.
26 F. Vigier, C. Coutanceau, F. Hahn, E. M. Belgsir, C. Lamy, *J. Electroanal. Chem.*, 2004, **563**, 81-89.